

Atomically resolved scanning tunneling microscopy images of dislocations

N. J. Zheng, I. H. Wilson, and U. Knipping

Department of Physics, Arizona State University, Tempe, Arizona 85287

D. M. Burt and D. H. Krinsley

Department of Geology, Arizona State University, Tempe, Arizona 85287

I. S. T. Tsong

Department of Physics, Arizona State University, Tempe, Arizona 85287

(Received 6 September 1988)

Freshly cleaved (001) surfaces of the mineral galena, PbS, were examined by scanning tunneling microscopy (STM) in vacuum. Atomically resolved images in real space showing areas with perfect order and with edge dislocations were obtained. The observed dislocations have Burgers vectors $a(1,0,0)$ and $\frac{1}{2}a(1,0,0)$ where [100] is the cleaving direction.

Scanning tunneling microscopy (STM), first introduced by Binnig, Rohrer, and co-workers,¹ has developed into a mature and powerful tool for surface-structure determination under both ultrahigh-vacuum and ambient-pressure conditions. Its most important advantage over other surface techniques is the capability to image in real space localized surface features with extremely high lateral ($\leq 2 \text{ \AA}$) and vertical ($\leq 0.01 \text{ \AA}$) resolution. Applications of STM to surface studies thus far can be broadly divided into two categories: (a) regularly ordered surface structure and (b) irregular surface structure. The former includes clean surfaces of single crystals, surface reconstructions, and specific reaction sites while the latter includes phase boundaries, atomic steps, and vacancies. The present work belongs to the second category and we report the first STM observations of edge dislocations on a PbS(001) single-crystal surface with atomic resolution.

Our single-crystalline PbS sample is the natural mineral galena, the principal ore of lead. It has the simple cubic structure of rock salt (NaCl) with a unit-cell edge of 5.94 \AA . It produces a perfect cleavage along the (001) planes. The cleavage surface shows striking inertness to air exposure, with no significant oxidation even after exposure to air for up to one hour.^{2,3} We prepared a fresh sample surface by cleaving the galena crystal with a razor blade in air along the (001) plane. The sample with the newly cleaved surface was then immediately transferred to the STM mounted in an ultrahigh-vacuum chamber. A vacuum of 10^{-5} Torr in the STM chamber was reached within 30 min of initial cleaving. Most of the STM images were taken in a vacuum of 10^{-7} Torr although we also conducted some experiments in air. Tunneling is not a problem with PbS since it is a low-band-gap (0.4 eV) polar semiconductor.

The STM used in this study was constructed on a six-in.-diam conflat flange with a two-stage spring and magnetic damping system for vibration isolation. The tunneling tip was made by electrolytic etching of a 0.25-mm tungsten wire in KOH. It is fully ultrahigh-vacuum compatible, but can also be operated in air if desired. The de-

tails of the instrument have been reported previously.⁴ The length scales on the x and y scanning directions were calibrated by imaging carbon atoms on the basal plane of a highly oriented pyrolytic graphite (HOPG) sample and the z direction was calibrated with a commercial electronic height gauge. The uncertainties in the calibrations were $\sim 5\%$ in x and y and $\sim 15\%$ in z directions. Thermal drift in the STM was periodically checked during the experiments. The drift rate was typically under 5 \AA per minute. The specific drift direction at any given time depended on whether the room temperature was drifting up or down at the time. Imaging was performed in a constant-current mode with a typical tunneling current of $\sim 0.8 \text{ nA}$. Tunneling voltage was typically between 0.3 and 0.8 V with the tip biased negatively. Tunneling voltage at 0.2 V or below generally resulted in a noisy scanning trace, a result which agrees with a bulk band gap of $\sim 0.4 \text{ eV}$ for PbS. In addition to imaging, we also measured the tunneling current, I_t , as a function of tip-sample separation s . From the slope of the $d \ln I_t / ds$ curve, the work function of the PbS(001) surface was determined to be about 3 eV in a vacuum of 1×10^{-7} Torr, close to previously reported values of $\sim 4.0 \text{ eV}$.⁵

Figure 1(a) shows an atomically resolved STM image of an ordered region of the PbS(001) surface obtained with the tip biased negatively at -0.5 V with respect to the sample, which is grounded. According to the calibration of our x - y PZT scanners, both Pb^{2+} and S^{2-} ions on the surface are imaged, with a unit-cell edge very close to 6 \AA , in agreement with the known value of 5.94 \AA . Interestingly, we could not image with the tip biased positively, i.e., probing filled states of the sample, the tunneling current being always noisy. Similar behavior has been noted by other STM workers in different samples.^{6,7} One explanation is the adsorption of an electronegative atom, such as S, on the probe tip, changing the local density of states near the Fermi level in such a way that lateral resolution is lost at tip positive but not at tip negative.⁷ This is a likely possibility since S atoms are known to evaporate from the PbS surface under vacuum⁵ and may become ad-

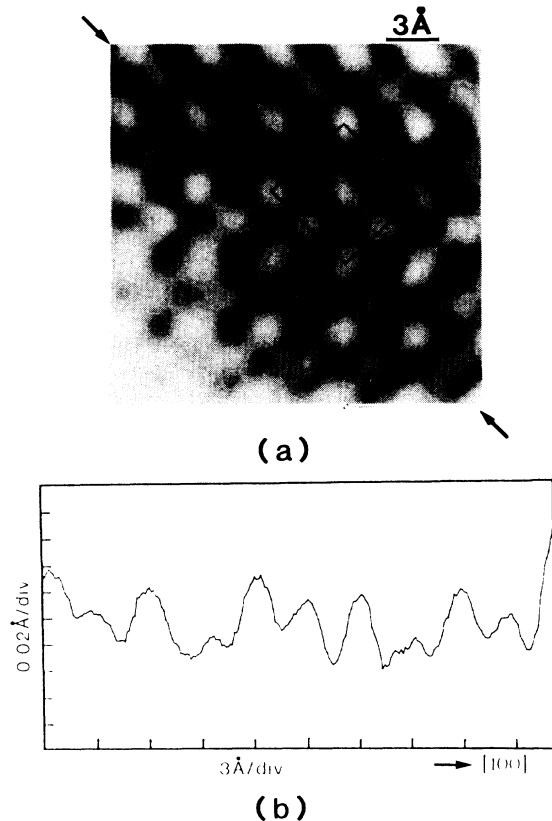


FIG. 1. (a) Atommally resolved STM gray-scale image of an ordered region of the PbS(001) surface. Bright spots indicate Pb^{2+} and S^{2-} ions on the surface. The unit-cell boundaries are marked. Tip bias at -0.5 V with sample grounded, tunnel current $I_t = 0.8$ nA. (b) Line trace showing height variations of surface ions along the $[100]$ direction, indicated by arrows in (a).

sorbed on the tip. Another explanation is that the PbS(001) surface is basically n -type under vacuum because of preferential evaporation of S atoms,⁵ thus pinning the Fermi level close to the conduction-band edge. Since STM probes the local density of states within a narrow energy window near the Fermi level, rather than the

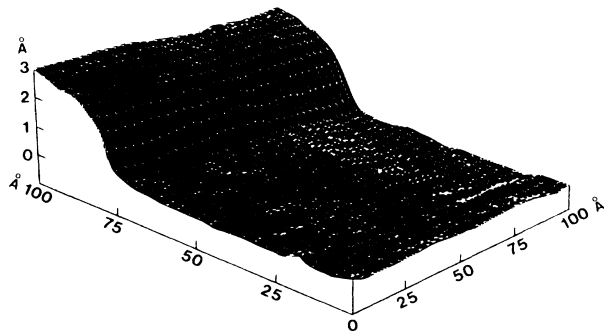


FIG. 2. Three-dimensional STM image of a single atomic step on the PbS(001) surface. The height of the step is 3 Å. Field of view is 100×100 Å². Tip bias at -0.5 V (sample grounded) and $I_t = 0.8$ nA.

actual atom positions, we can probe the empty states in the conduction band with the tip negative, but not the filled states when the tip is biased positively. This explanation is less satisfactory since the band gap of PbS is only 0.4 eV and one can expect to obtain a tunneling image if one increases the positive bias on the tip.

Another interesting feature is the distinct height variations in the two ionic species as shown in the trace in Fig. 1(b). This is probably due to the heavier concentration of charge density around the S^{2-} ions compared to the charge density surrounding the Pb^{2+} ions on (001) planes of PbS,⁸ which has the effect of causing the STM to "see" the S^{2-} ions as more protruding on the PbS(001) surface.⁹

When examined under an optical microscope, the (001) cleavage surface of a galena crystal often shows a large number of steps, most of which are along $[100]$ and $[110]$ directions. These cleavage steps are a good indication of the existence of dislocations on the PbS(001) surface. During the cleavage process, if a cleavage front intersects a dislocation with Burgers vector \mathbf{b} , a step with height $\mathbf{b} \cdot \mathbf{n}$

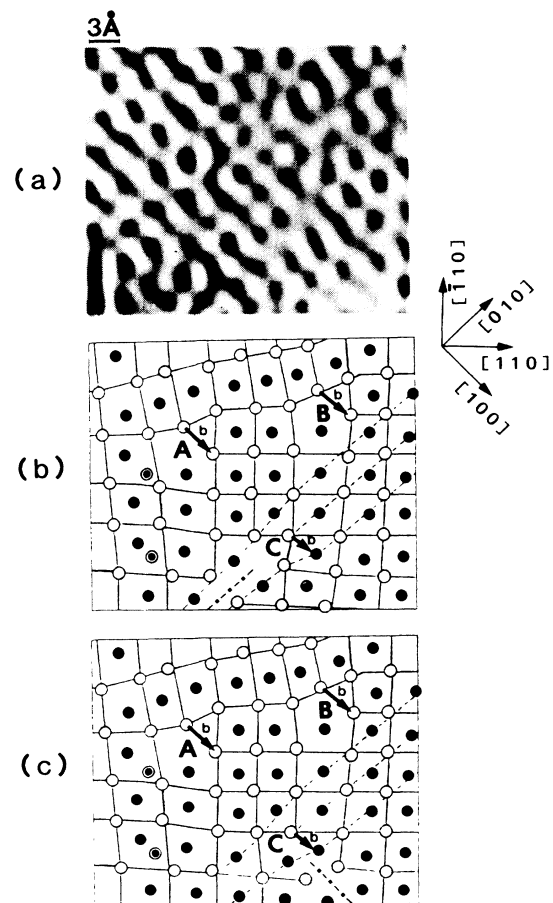


FIG. 3. (a) Atommally resolved STM gray-scale image of a region of imperfections on the PbS(001) surface. Bright spots indicate Pb^{2+} and S^{2-} ions on the surface. Tip bias at -0.5 V (sample-grounded) and $I_t = 0.8$ nA. (b) and (c) Two different models of the STM image (a) showing edge dislocations at positions A, B, and C. The Burgers vectors are also shown. \circ , Pb^{2+} ion; \bullet , S^{2-} ion; and \odot , interstitial atom.

occurs.¹⁰ (\mathbf{n} is the unit vector normal to the cleavage surface.) The primary glide system in PbS is $\langle 101 \rangle \{001\}$. The *smallest* Burgers vector of this type of dislocation is $\frac{1}{2}a(1,0,1)$, which will result in a step of 3 Å, i.e., half of the unit-cell edge, on the (001) cleavage surface. Figure 2 shows a three-dimensional STM image of an atomic step with a height of 3 Å. From a large area ($500 \times 500 \text{ \AA}^2$) scan, we chose a flat region free of steps for atomic-resolution scans. Figure 3(a) shows a small $35 \times 30 \text{ \AA}^2$ region with a high concentration of dislocations. In order to clarify the dislocation structures, we mark the position of the bright spots in Fig. 3(a) with open and filled circles representing the two ions, i.e., Pb^{2+} and S^{2-} , as shown in Figs. 3(b) and 3(c). Edge dislocations emerging from positions A, B, and C can clearly be seen. Burgers vectors \mathbf{b} are indicated by arrows. We refrain from marking the surface ion positions directly on the STM gray-scale image of Fig. 3(a) for the sake of clarity. However, if a transparency is made in Figs. 3(b) and 3(c) and placed directly on top of Fig. 3(a), one can see that the circled positions match the bright spots of the image perfectly.

The edge dislocations at positions A and B [shown in both Figs. 3(b) and 3(c)] have the same Burgers vector $a(1,0,0)$ as determined by the Burgers loop.¹¹ Two extra (110) and $(\bar{1}\bar{1}0)$ planes terminate at these two positions, which in turn means a slip along [110] and $[\bar{1}\bar{1}0]$ directions, respectively, by an amount of $a/2$. The resultant Burgers vector is thus $a(1,0,0)$. The edge dislocation at position C has a Burgers vector of $\frac{1}{2}a(1,0,0)$. Two possible ionic arrangements around the C dislocation are shown in Figs. 3(b) and 3(c). Ideally, one should be able to identify the Pb^{2+} and S^{2-} ions according to their height difference as shown in Fig. 1(b), thus resolving the issue as to whether Fig. 3(b) or 3(c) correctly depicts the ionic arrangement. Unfortunately, it appears that in this highly defective region, the distribution of charge density is modified to such an extent that a clear distinction of the ions by height difference is very difficult.

The C dislocation in Fig. 3(b) is caused by the precipitation of vacancies on the (100) plane, indicated by the dot-dashed line, creating an electrostatic stacking fault of

high energy with like ions on both sides of the dot-dashed line. The energy of the stacking fault can be released by an offset of $\frac{1}{2}a(0,1,0)$, according to Amelinckx,¹² which changes the Burgers vector from $\frac{1}{2}a(1,0,0)$ to $\frac{1}{2}a(1,1,0)$. So the ionic arrangement as depicted in Fig. 3(b) is most likely energetically unfavorable.

The C dislocation shown in Fig. 3(c) is caused by a glide along the [100] direction by $a/2$. The ionic arrangement also has adjacent like charges as indicated by the dot-dashed line. However, this configuration, once formed, cannot be removed by the offset mechanism as in the case of Fig. 3(b). We believe that Fig. 3(c) is a correct description of the STM image shown in Fig. 3(a). This type of dislocation is similar to the prismatic dislocation found in cubic crystals on the (001) plane if an indentation is made on the (100) plane along the [100] direction.^{13,14}

There is another possibility that the C dislocation has a component along the [001] direction of $\frac{1}{2}a(0,0,1)$, which results in the actual Burgers vector being $\frac{1}{2}a(1,0,1)$. However, this would give rise to a step with a height of half of the unit-cell edge, i.e., 3 Å, as we have mentioned earlier. Such a step was neither observed in the STM image of Fig. 3(a) nor in a larger area ($500 \times 500 \text{ \AA}^2$) scan which showed that regions adjacent to the dislocations were atomically flat.

We note that all Burgers vectors observed in the STM image shown in Fig. 3(a) are along the [100] direction which is also the direction of cleaving. It is likely that the dislocations observed on the PbS(001) cleaved surface is associated with the cleaving procedure.

The results of this investigation illustrate the capability of STM in obtaining images with atomic resolution on dislocations on a crystal surface, thus demonstrating that STM can be usefully applied to study imperfections and deformation processes in materials.

This work was supported in part by the U.S. Army Research Office under Contract No. DAAL03-88-K-0098 and by the Arizona State University vice president for research.

¹G. Binnig and H. Rohrer, IBM J. Res. Dev. **30**, 355 (1986), and references therein.

²A. N. Buckley and R. Woods, Appl. Surf. Sci. **17**, 401 (1984).

³J. A. Tossell and D. J. Vaughan, Can. Mineral. **25**, 381 (1987).

⁴N. J. Zheng, U. Knipping, I. S. T. Tsong, W. T. Petuskey, and J. C. Barry, J. Vac. Sci. Technol. A **6**, 457 (1988).

⁵T. Grandke and M. Cardona, Surf. Sci. **92**, 385 (1980).

⁶M. D. Pashley, K. W. Haberern, W. Friday, J. M. Woodall, and P. D. Kirchner, Phys. Rev. Lett. **60**, 2176 (1988).

⁷R. M. Tromp, E. J. van Loenen, J. E. Demuth, and N. D. Lang, Phys. Rev. B **37**, 9042 (1988).

⁸R. Dalven, in *Solid State Physics*, edited by H. Ehrenreich, F. Seitz, and D. Turnbull (Academic, New York, 1973), Vol. 28, p. 179.

⁹J. Tersoff and D. R. Hamann, Phys. Rev. B **31**, 805 (1985).

¹⁰S. Amelinckx, *The Direct Observation of Dislocations*, Solid State Physics Suppl. 6 (Academic, New York, 1964), p. 50.

¹¹J. P. Hirth and J. Lothe, *Theory of Dislocations* (McGraw-Hill, New York, 1968).

¹²S. Amelinckx, in *Mechanical Properties of Engineering Ceramics*, edited by W. W. Kriegel and H. Palmour III (Interscience, New York, 1961), p. 25; *The Direct Observation of Dislocations*, Solid State Physics, Suppl. 6 (Academic, New York, 1964).

¹³F. Seitz, Phys. Rev. **79**, 723 (1950).

¹⁴F. R. N. Nabarro, *Theory of Crystal Dislocations* (Oxford Univ. Press, London, 1967).

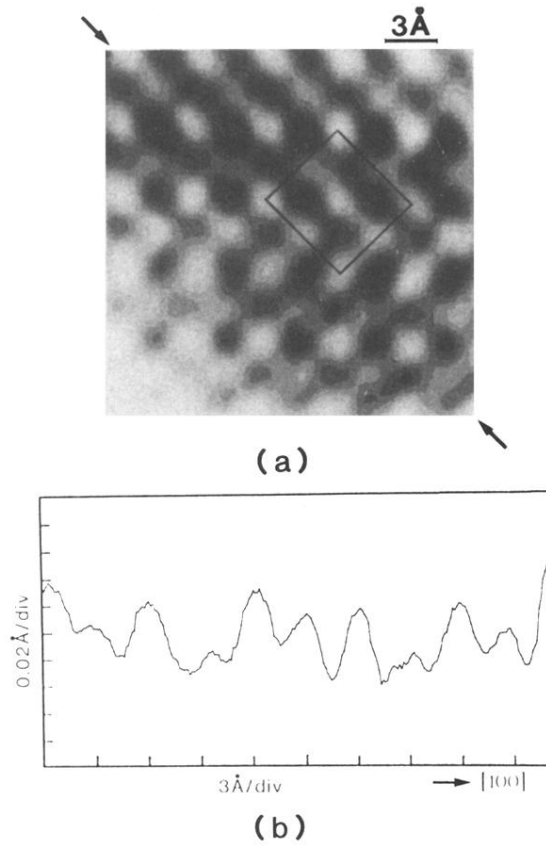


FIG. 1. (a) Atommically resolved STM gray-scale image of an ordered region of the PbS(001) surface. Bright spots indicate Pb^{2+} and S^{2-} ions on the surface. The unit-cell boundaries are marked. Tip bias at -0.5 V with sample grounded, tunnel current $I_t = 0.8$ nA. (b) Line trace showing height variations of surface ions along the [100] direction, indicated by arrows in (a).

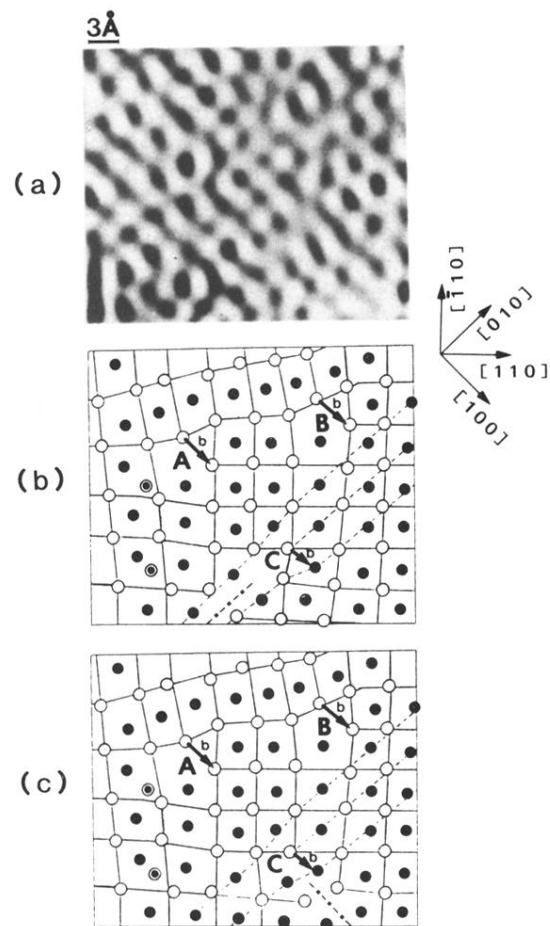


FIG. 3. (a) Atomically resolved STM gray-scale image of a region of imperfections on the PbS(001) surface. Bright spots indicate Pb^{2+} and S^{2-} ions on the surface. Tip bias at -0.5 V (sample-grounded) and $I_t = 0.8$ nA. (b) and (c) Two different models of the STM image (a) showing edge dislocations at positions A, B, and C. The Burgers vectors are also shown. \circ , Pb^{2+} ion; \bullet , S^{2-} ion; and \odot , interstitial atom.